g-factors in quantum dots

Craig Pryor
Dept. of Physics and Astronomy
University of Iowa

With: Michael Flatté, Joseph Pingenot, Amrit De

supported by DARPA/ARO DAAD19-01-1-0490

g-factors in quantum dots

- bulk g-factors
- g-factors in self-assembled quantum dots
- g-factors nanowhisker dots
- modulation by E-fields, g-TMR

With: Michael Flatté, Joseph Pingenot, Amrit De

Pryor and Flatté PRL 96, 026804

free electron

$$\vec{\mu}_s = -\frac{g}{2}\,\mu_B\,\vec{\sigma}$$

$$g = 2 + O(1/137)$$

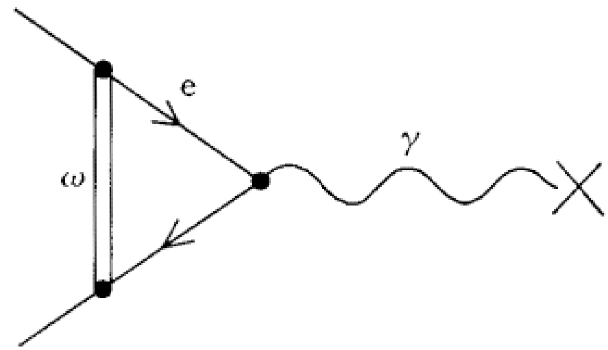

$$H = \frac{1}{2m}\left(\vec{P} + \frac{e}{c}\vec{A}\right)^2 + \frac{g}{2}\,\mu_B\,\vec{\sigma}\cdot\vec{B}$$

band electron

$$\vec{\mu}_s = -\frac{g}{2}\,\mu_B\,\vec{\sigma}$$

$$g = 2 - |something|$$

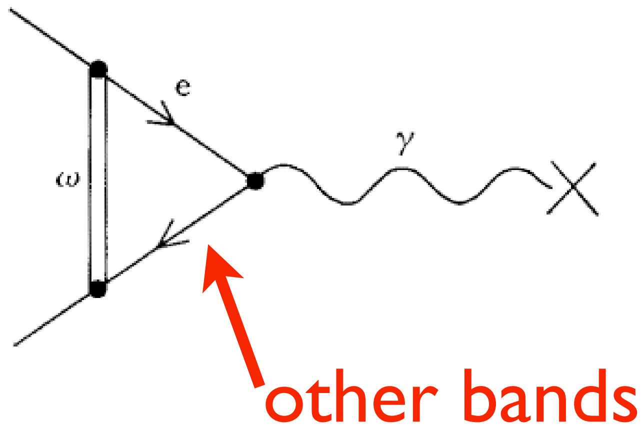

$$H = \frac{1}{2m}\left(\vec{P} + \frac{e}{c}\vec{A}\right)^2 + \frac{g}{2}\,\mu_B\,\vec{\sigma}\cdot\vec{B}$$

atomic Landé g-factor

orbital l + spin s $\Rightarrow$ total j

$$g = 1 + \frac{j(j+1) + s(s+1) - l(l+1)}{2j(j+1)}$$

Bloch state g-factors (zone center)

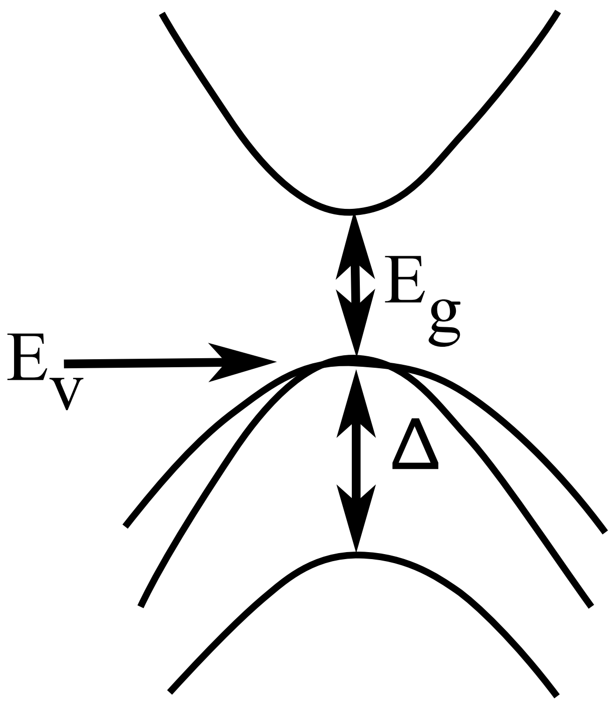

$$g = 2 : \; l = 0, \; s = \frac{1}{2}, \; j = \frac{1}{2}$$

$$g = 4/3 : \; l = 1, \; s = \frac{1}{2}, \; j = \frac{3}{2}$$

$$g = 2/3 : \; l = 1, \; s = \frac{1}{2}, \; j = \frac{1}{2}$$

$$g = 1 + \frac{j(j+1) + s(s+1) - l(l+1)}{2j(j+1)}$$

bulk semiconductor g-factors (k.p)

$$\boldsymbol{H} = \frac{1}{2m}\left(\vec{P} + \frac{e}{c}\vec{A}\right)^2 + \frac{g}{2}\,\mu_B\,\vec{\sigma}\cdot\vec{B}$$

$$\psi(\boldsymbol{r}) = \sum_{i,s} c_{i,s} e^{i\boldsymbol{k}\cdot\boldsymbol{r}} u_{i,s}(\boldsymbol{r})$$

$$g = 2 - \frac{2i}{m}\sum_{k\neq n}\frac{\langle n\,|p_x|\,k\rangle\,\langle k\,|p_y|\,n\rangle - \langle n\,|p_y|\,k\rangle\,\langle k\,|p_x|\,n\rangle}{E_n^0 - E_k^0}$$

Roth et al. Phys. Rev **114**, 90 (1959)

bulk semiconductor g-factors (k.p)

electron magnetic moment

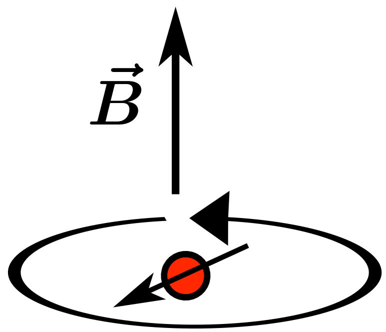

$$\vec{\mu}_s = -\frac{g}{2}\,\mu_B\,\vec{\sigma}$$

bulk semiconductor

$$g = 2 - \frac{2\,E_p\,\Delta}{3E_g(E_g+\Delta)}$$

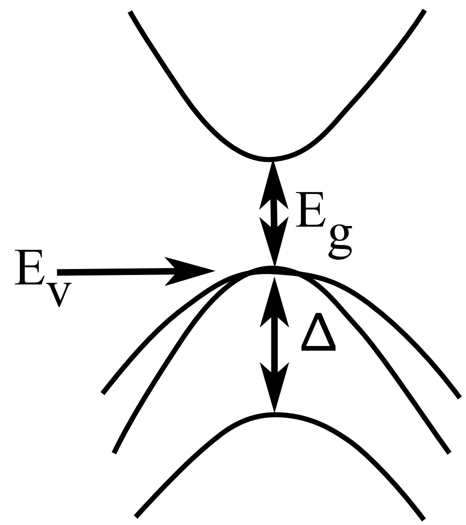

Roth et al. Phys. Rev **114**, 90 (1959)

bulk semiconductor g-factors (k.p)

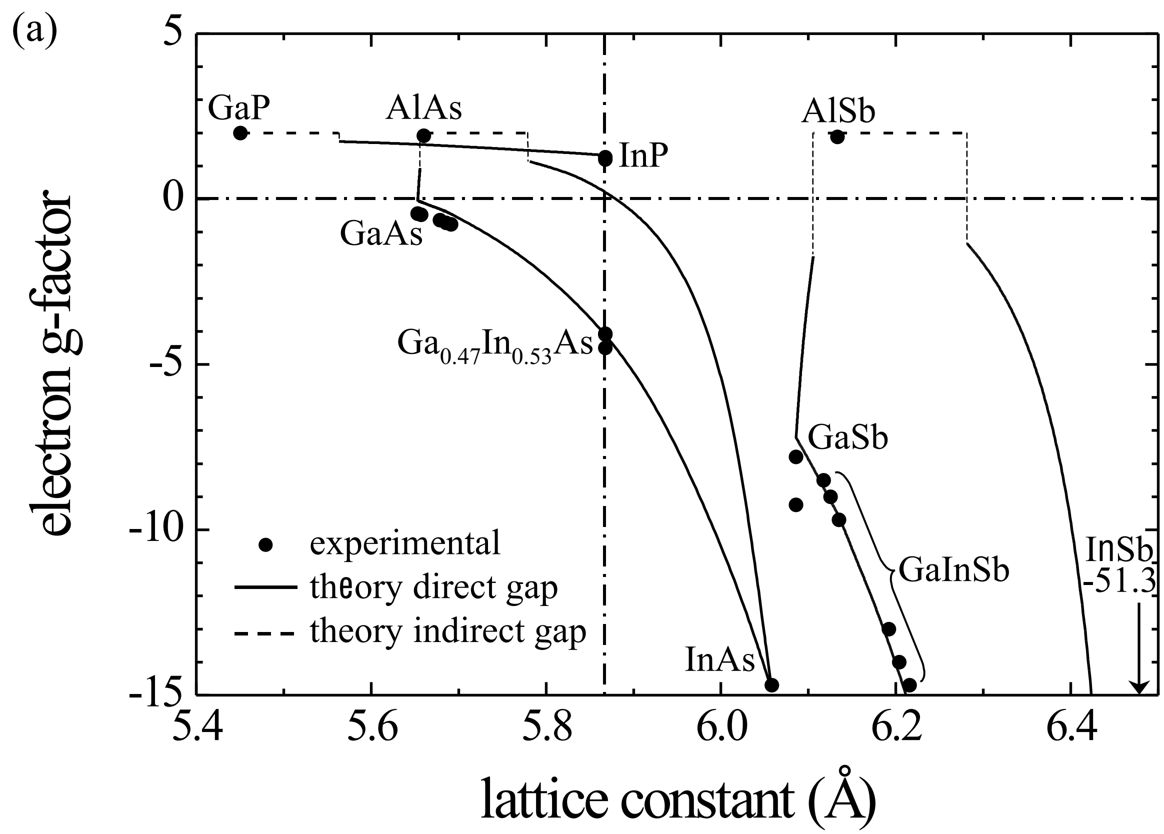

Kosaka et al. Electronics Letters **37**, 464

strained InAs/GaAs quantum dots

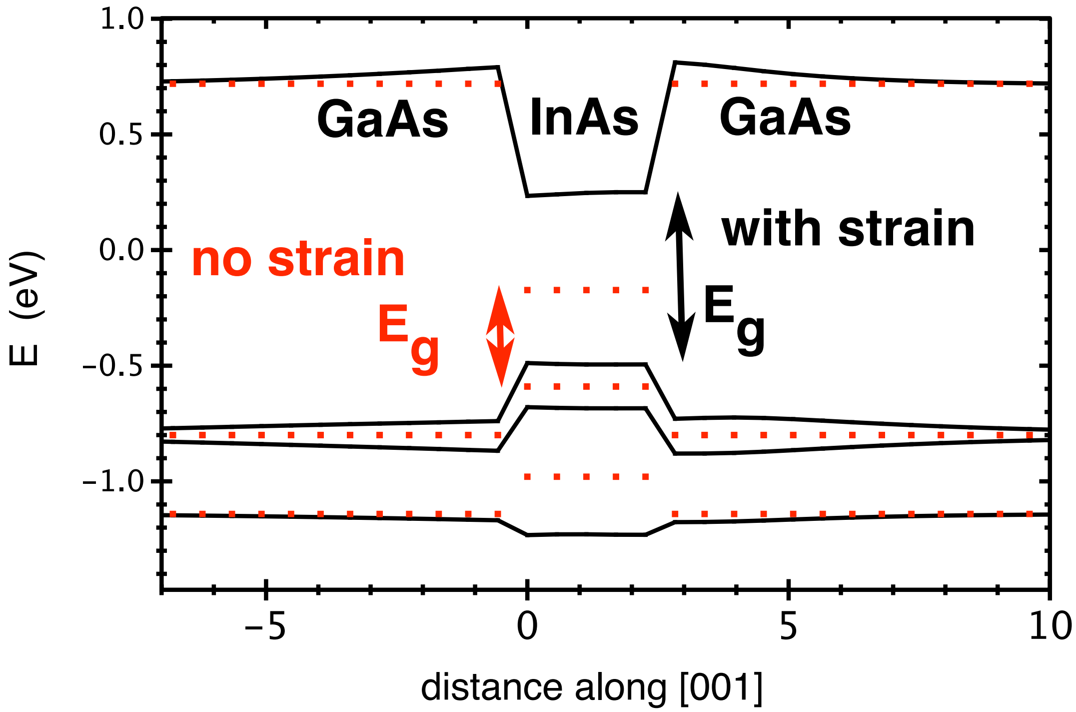

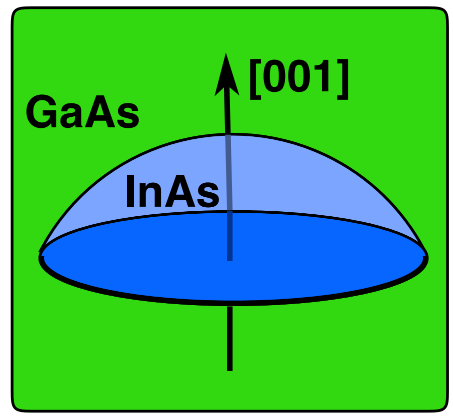

$$g = 2 - \frac{2\ E_p\ \Delta}{3E_g(E_g + \Delta)}$$

strained InAs/GaAs quantum dots

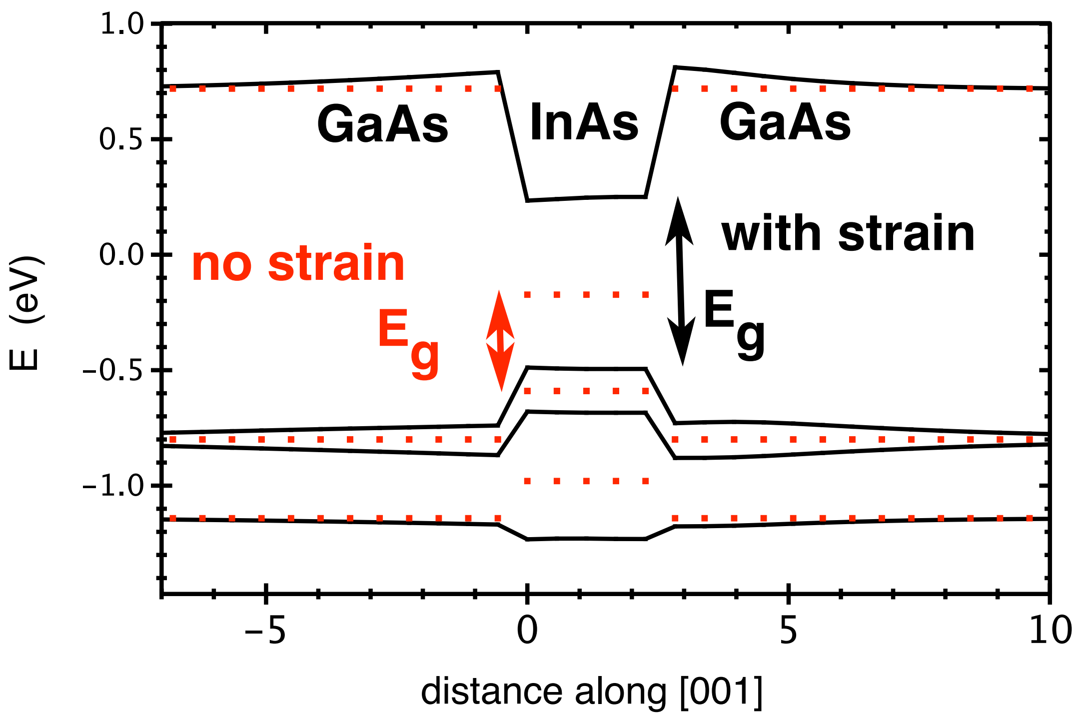

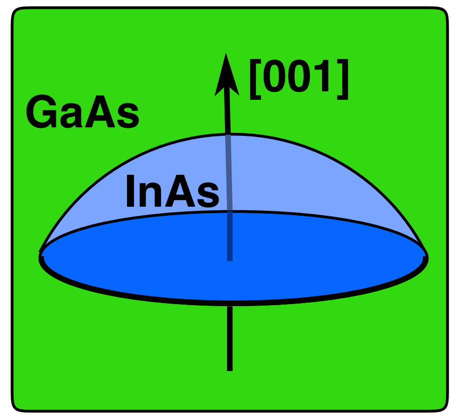

unstrained: $g_{InAs} = -14.6$

strained: $g_{InAs} \approx -6.1$

confinement: $g_{InAs} \approx -0.55$

$$g = 2 - \frac{2\ E_p\ \Delta}{3E_g(E_g + \Delta)}$$

quantum dot k.p calculations

- calculate strain using finite elements
- Schrödinger equation: $H\psi(r) = E\psi(r)$
- $\psi(r)$ is an 8-component vector, and H is an 8x8 matrix with elements like $A = E_c(r) - \frac{\hbar^2}{2m_0}\left(\partial_x^2 + \partial_y^2 + \partial_z^2\right) + a_c(r)\sum_i e_{ii}(r)$
- put system on a grid: $\partial_x^2 \psi_i(r) \rightarrow \frac{\psi_i(r + \epsilon\hat{x}) + \psi_i(r - \epsilon\hat{x}) - 2\psi_i(r)}{\epsilon^2}$
- solve for eigenvalues and eigenvectors as a sparse matrix problem using the Lanczos algorithm

nanostructures in B-fields

coupling to envelope (c.f. lattice gauge theory)

$$\frac{\psi(\vec{r}+\epsilon\hat{x})-\psi(\vec{r}-\epsilon\hat{x})}{2\epsilon} \to \frac{\psi(\vec{r}+\epsilon\hat{x})U_x(\vec{r})-\psi(\vec{r}-\epsilon\hat{x})U_x^\dagger(\vec{r}-\epsilon\hat{x})}{2\epsilon}$$

$$U_x(\vec{r})U_y(\vec{r}+\epsilon\hat{x})U_x^\dagger(\vec{r}+\epsilon\hat{y})U_y^\dagger(\vec{r}) = \exp(i\epsilon^2 B_\perp e/\hbar)$$

Pauli term for Bloch function spin

$$H_s = \frac{\mu_B}{2}\vec{B}\cdot\begin{pmatrix} 2\vec{\sigma} & 0 & 0 \\ 0 & \frac{4}{3}\vec{J} & 0 \\ 0 & 0 & \frac{2}{3}\vec{\sigma} \end{pmatrix}$$

g-factors in spherical dots

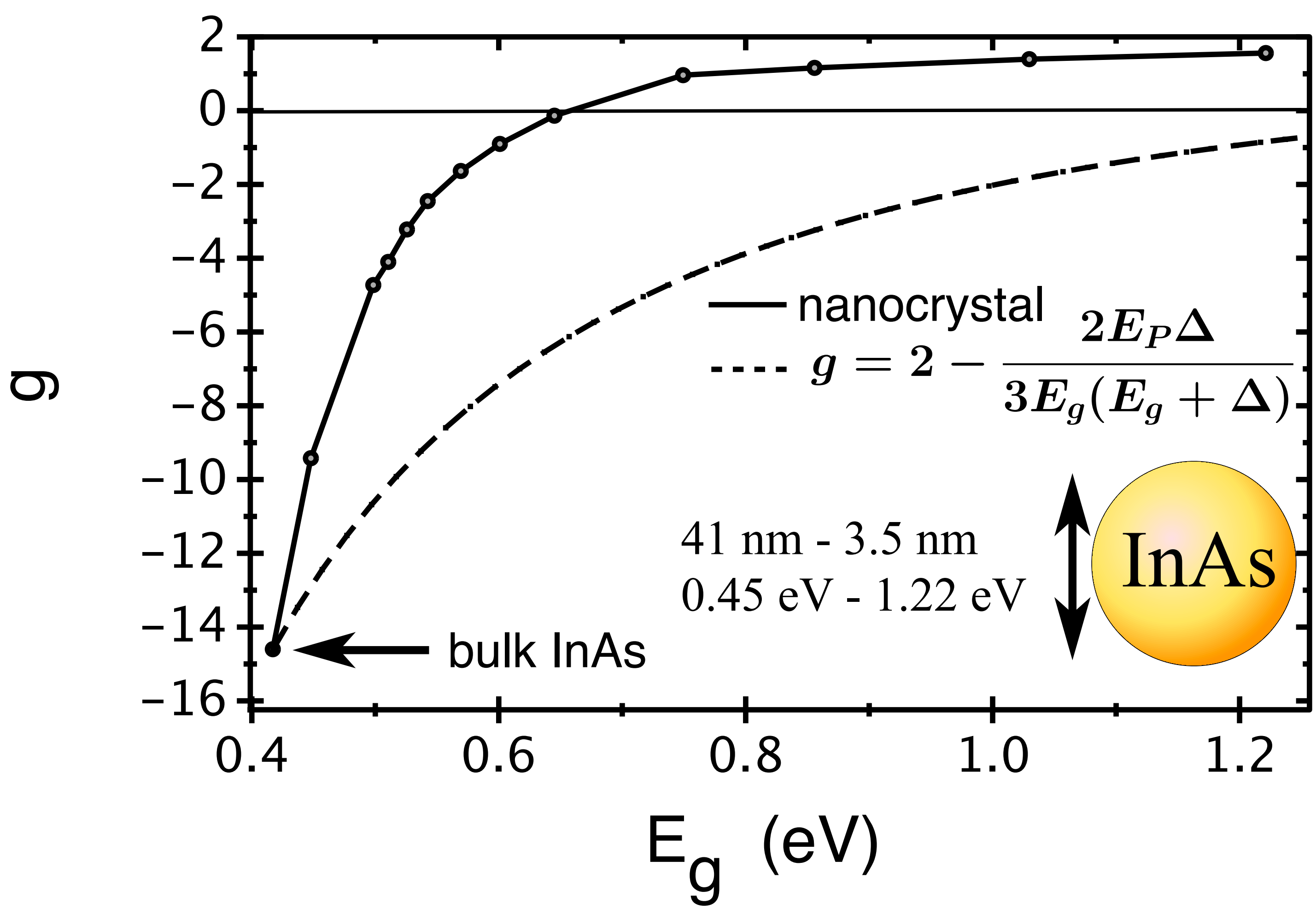

angular momentum quenching

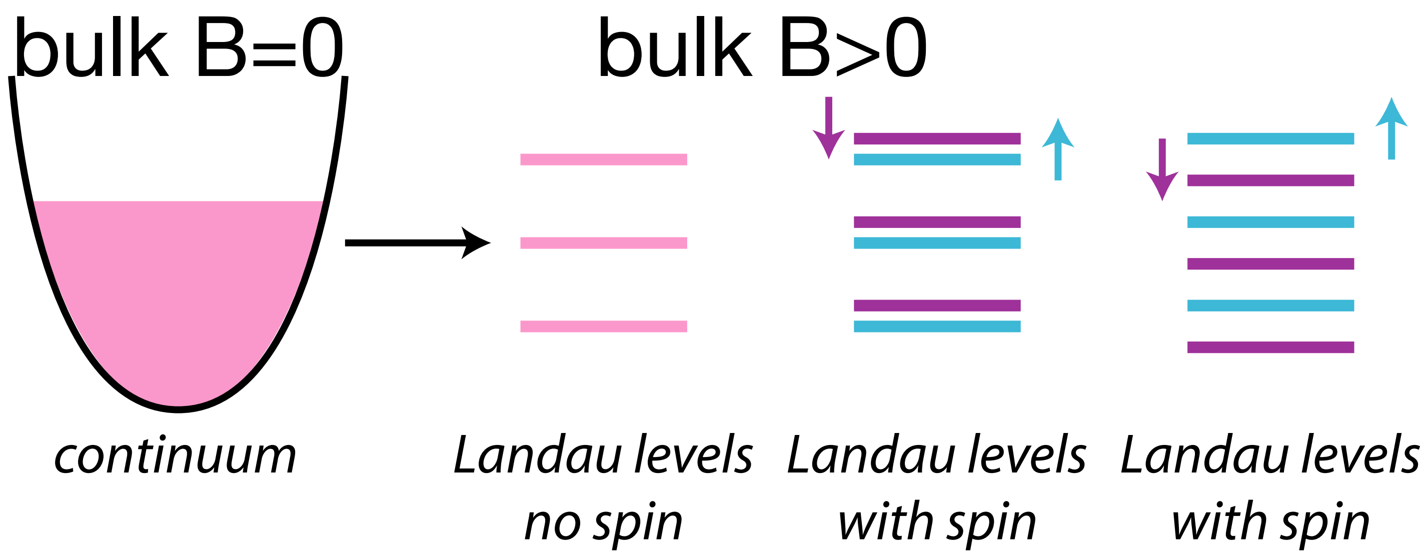

$$H = \frac{1}{2m}\left(\vec{P} + \frac{e}{c}\vec{A}\right)^2 + \frac{g}{2}\,\mu_B\,\vec{\sigma}\cdot\vec{B} + \frac{\hbar}{4m^2c^2}\,\frac{1}{r}\,\frac{dV}{dr}$$

$$g = 2 - \frac{2E_P\,\Delta}{3E_g(E_g+\Delta)}$$

Roth, Lax, Zwerdling, PR 114, 90 (1959)

angular momentum quenching

bulk B=0 | bulk B>0

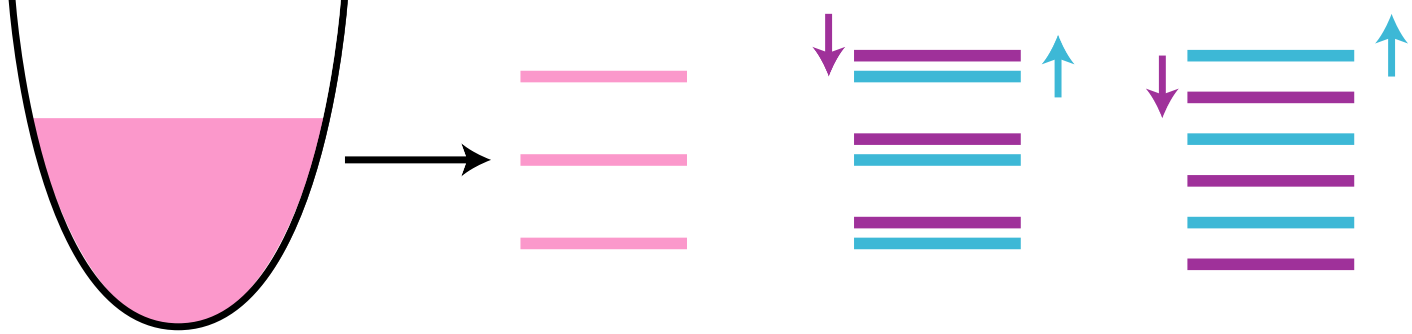

continuum

Landau levels no spin

Landau levels with spin

Landau levels with spin and spin-orbit (electron g<2)

$$g = 2 - \frac{2E_P \Delta}{3E_g(E_g + \Delta)}$$

Roth, Lax, Zwerdling, PR 114, 90 (1959)

Van Vleck, 1932

atom

angular momentum J: 2J+1 states

spin-orbit (vacuum)

$g < 2$

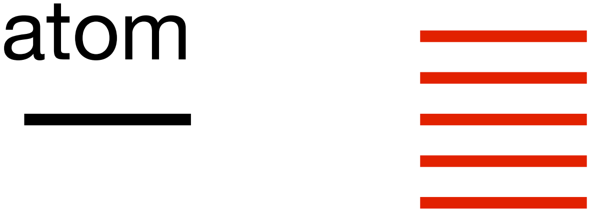

crystal field splitting (solid)

$g = 2$

quenching of angular momentum

InAs/GaAs dots

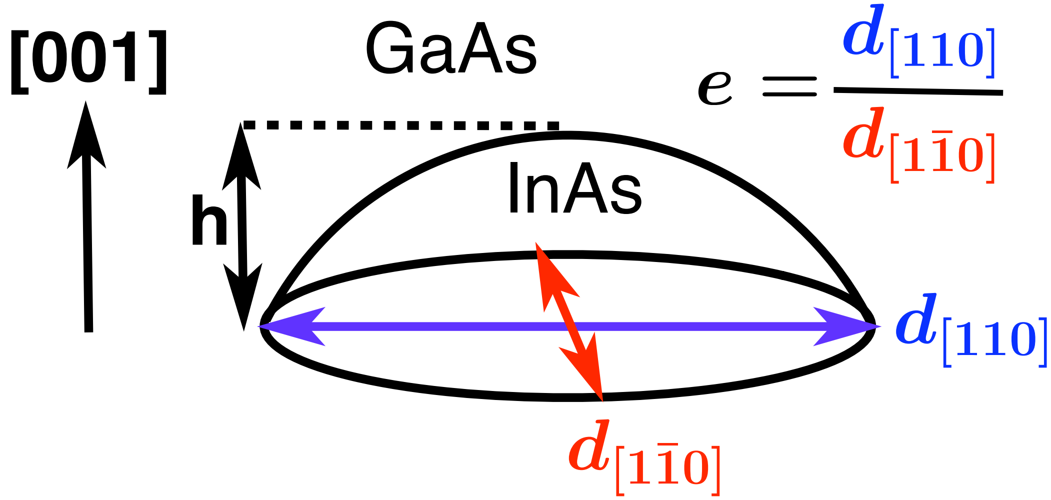

$$e = \frac{d_{[110]}}{d_{[1\bar{1}0]}}$$

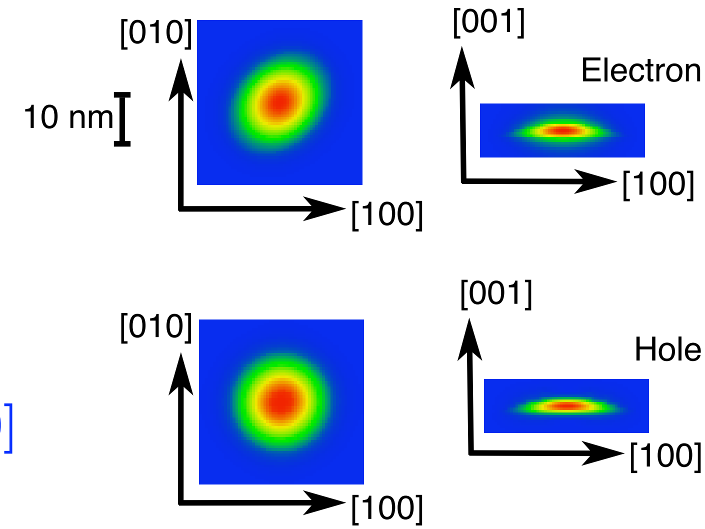

g-factors in InAs/GaAs dots

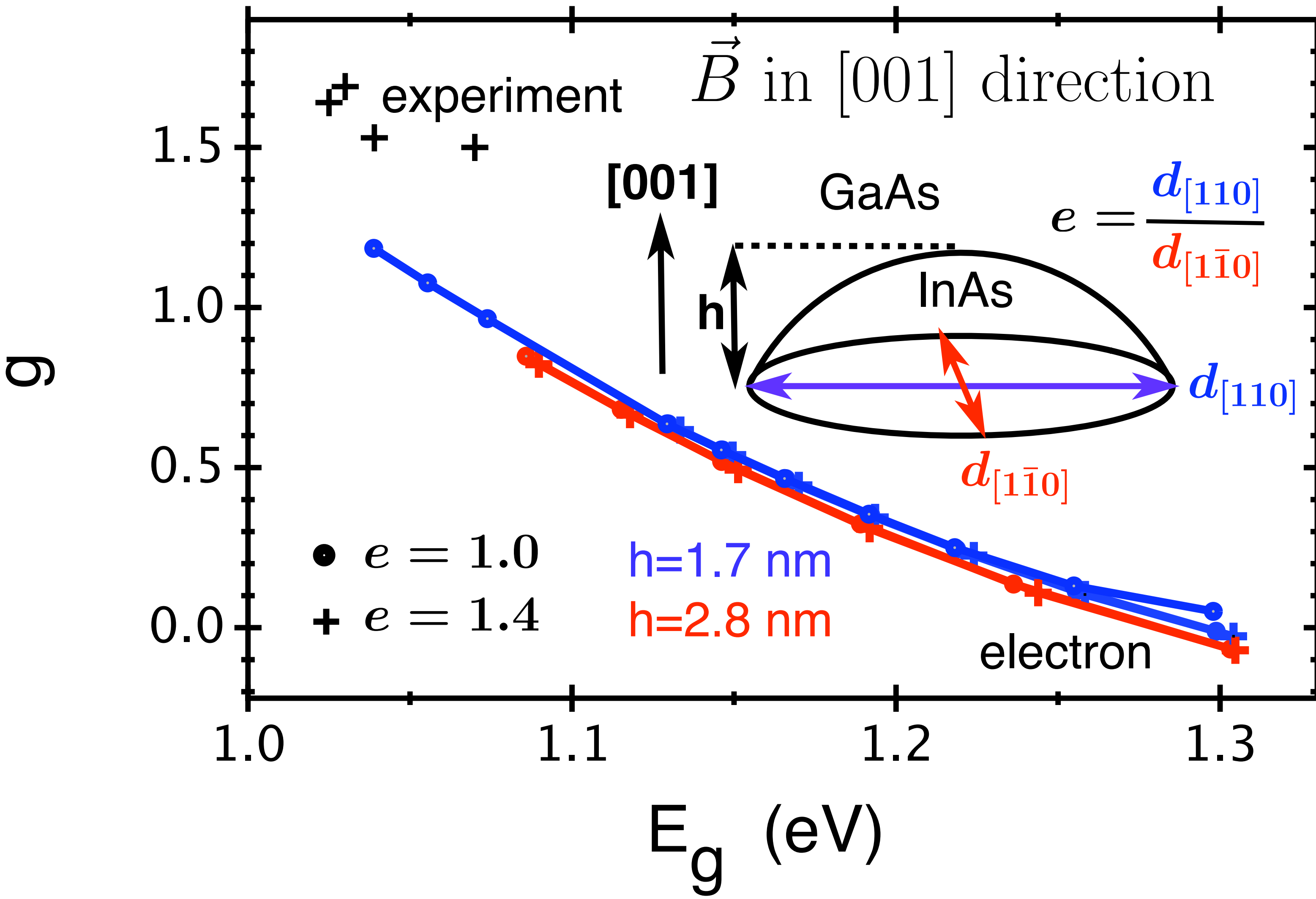

experiment: G. Medeiros-Ribeiro et al. Appl. Phys. A (2003)

in-plane g-factors

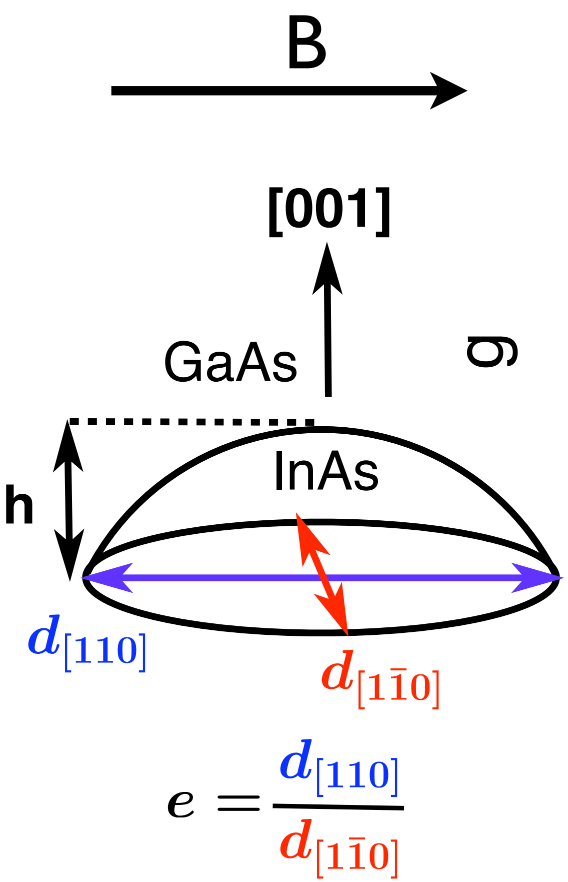

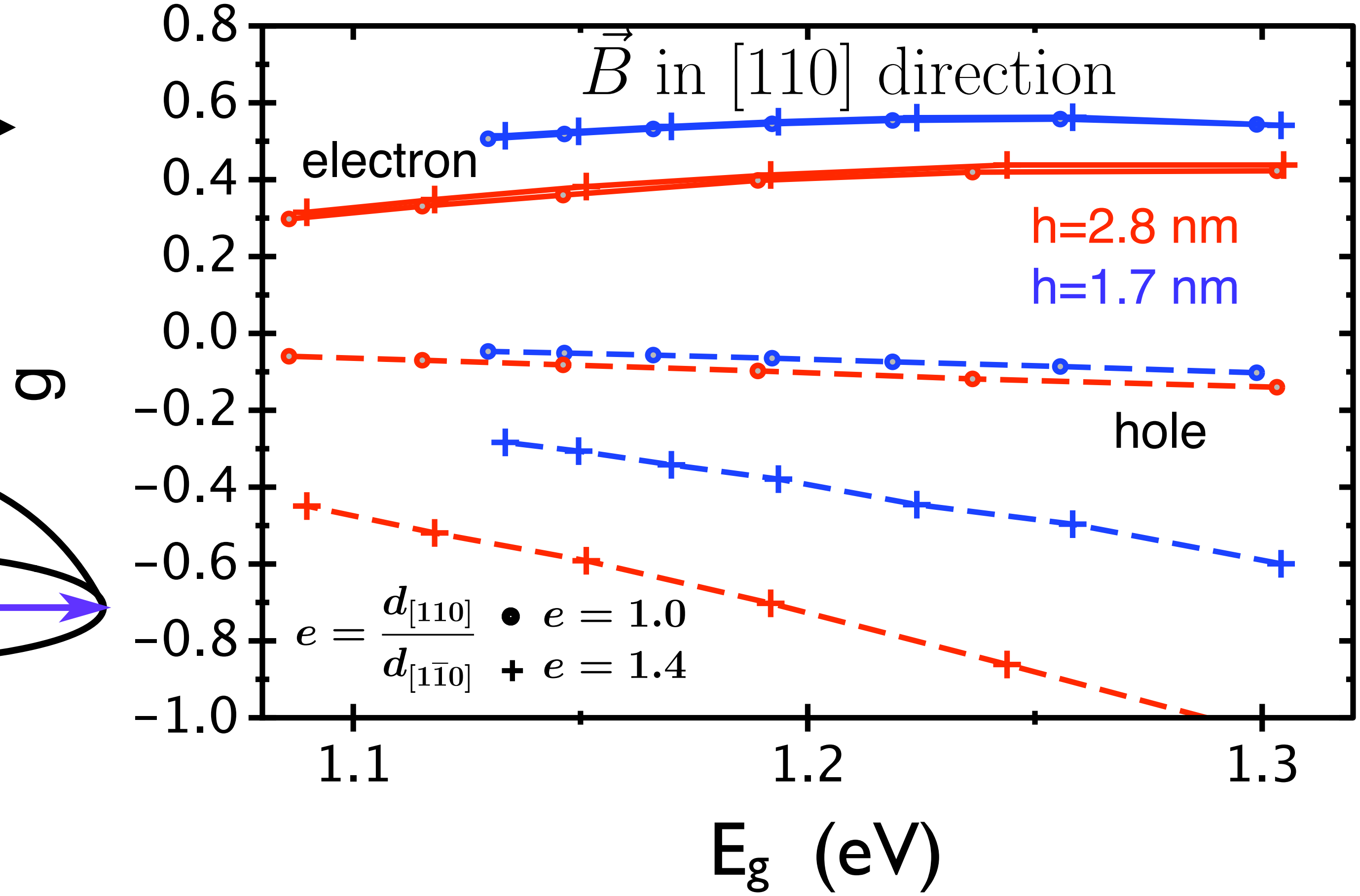

whisker dots

Amrit De

- quantum well inside a nanowhisker

N. Panev et al, APL, 83, 2238 (2003)

- resonant-magneto-tunneling spectroscopy

M. T. Bjork, et al, PRB 72,201307,(R) (2005)

- Hexagonal cross-section, <111> orientation, wurtzite

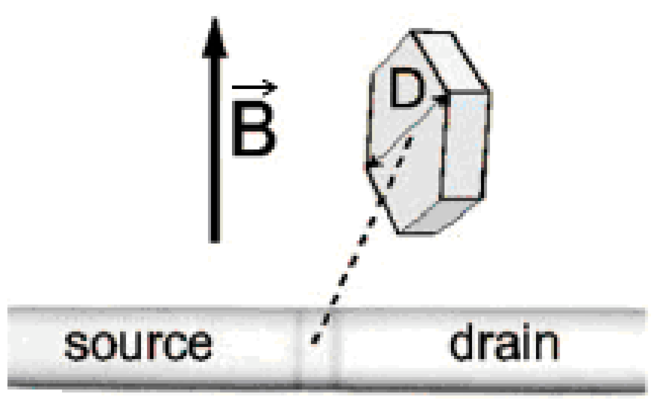

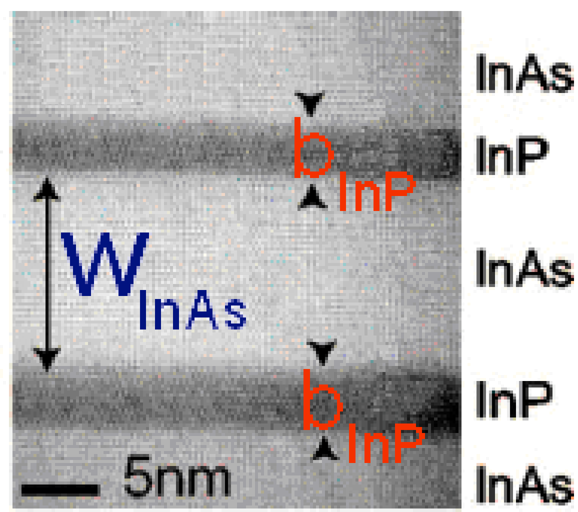

whisker orientation

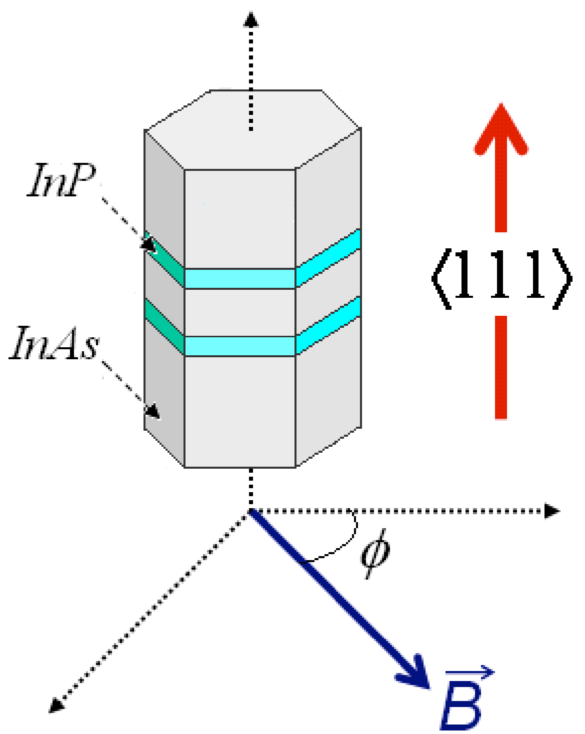

b_{InP} = 2.6 nm W_{InAs} = 6 nm D = 40 nm

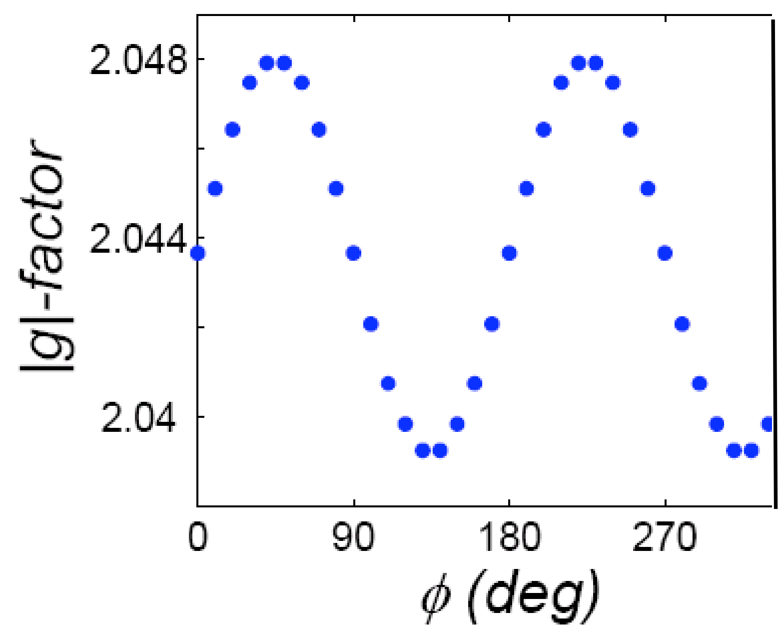

theory-vs-experiment

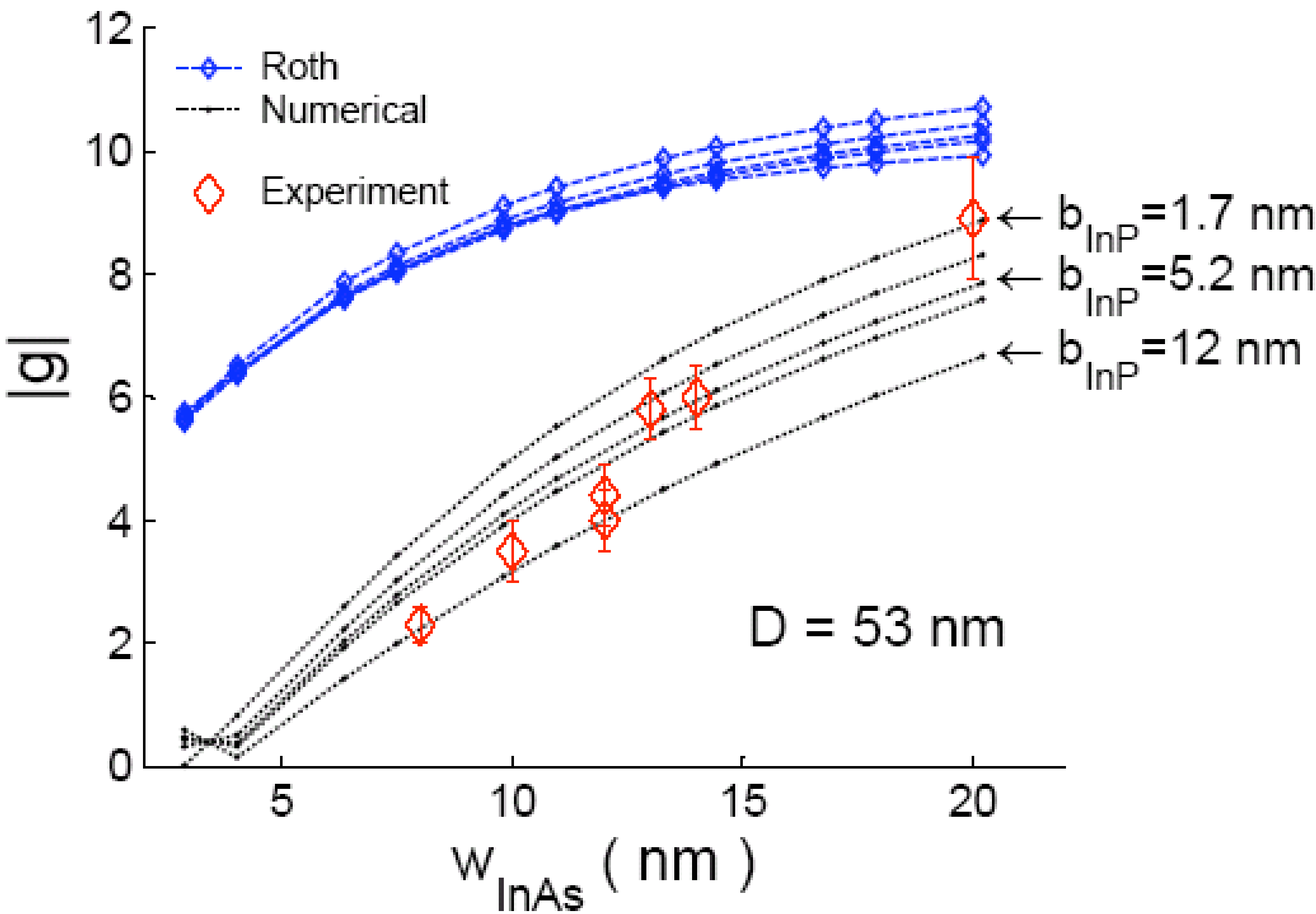

theory-vs-experiment

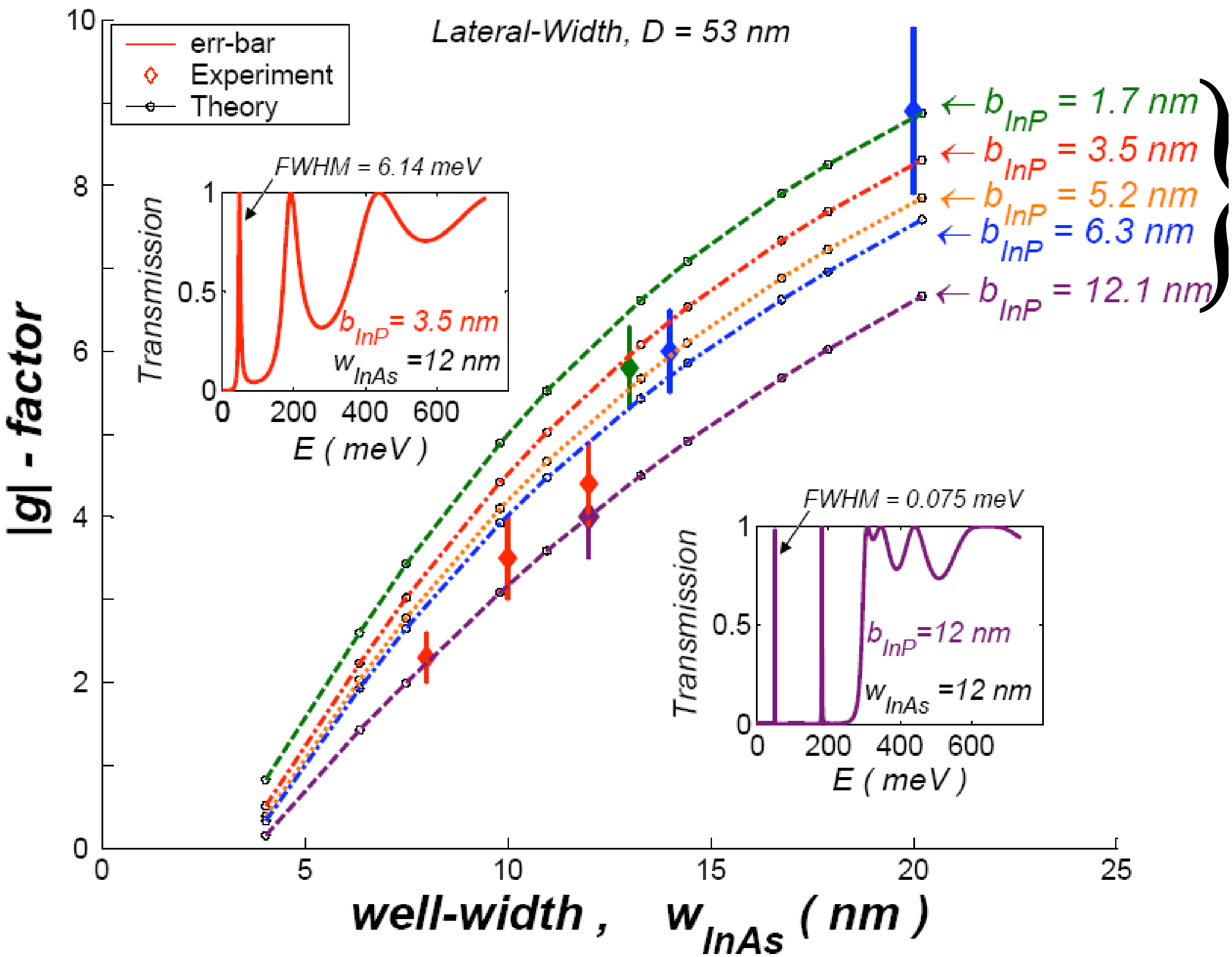

coupling to leads

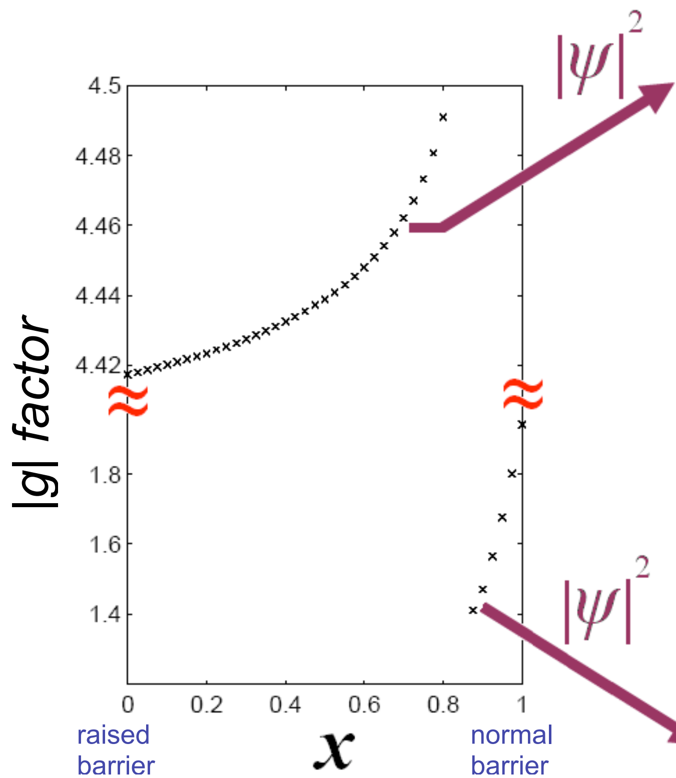

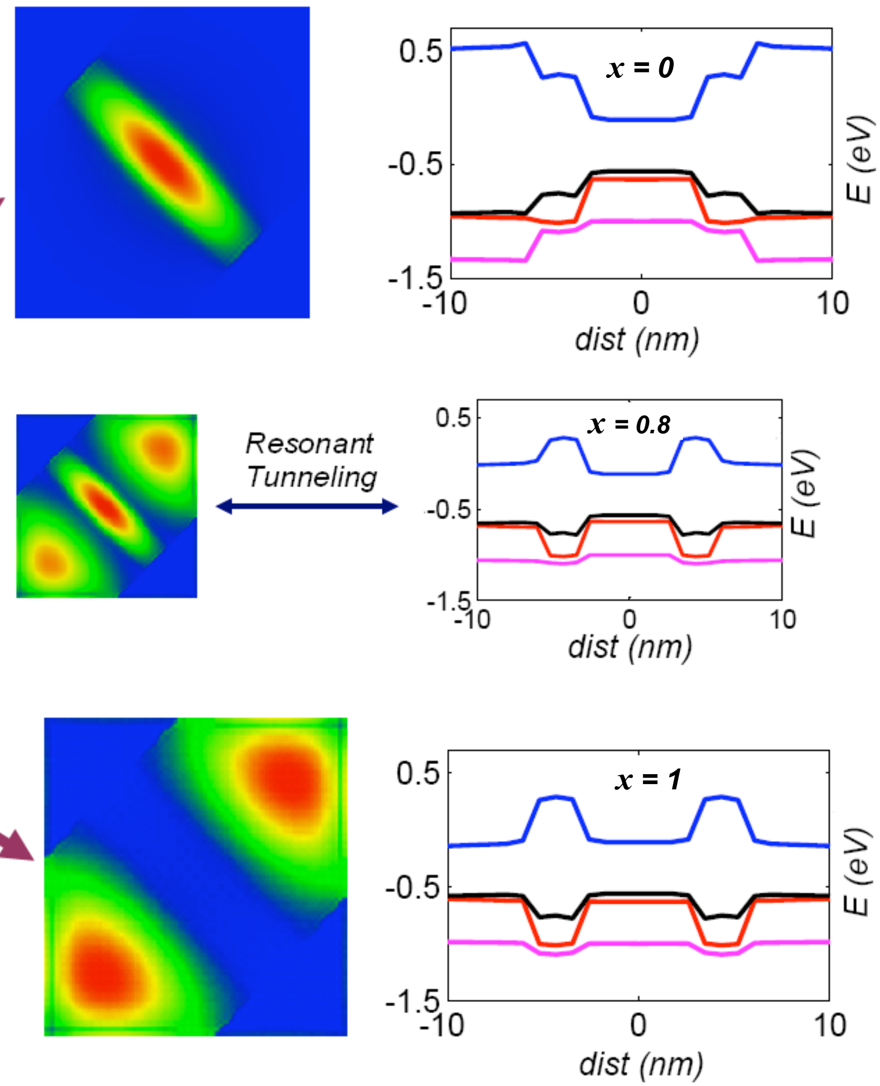

$$E_{g(v)}^{(artificial\text{-}InAs)} = x\, E_{g(v)}^{(InAs)} + (1-x)\, E_{g(v)}^{(InP)}$$

whisker dots

- clean geometry and composition allows better comparison than for self-assembled dots
- much closer to experiment than Roth formula
- coupling to leads alters g
- wurtzite structure still a complication

electrical control of g-factors, g-TMR

Joseph Pingenot

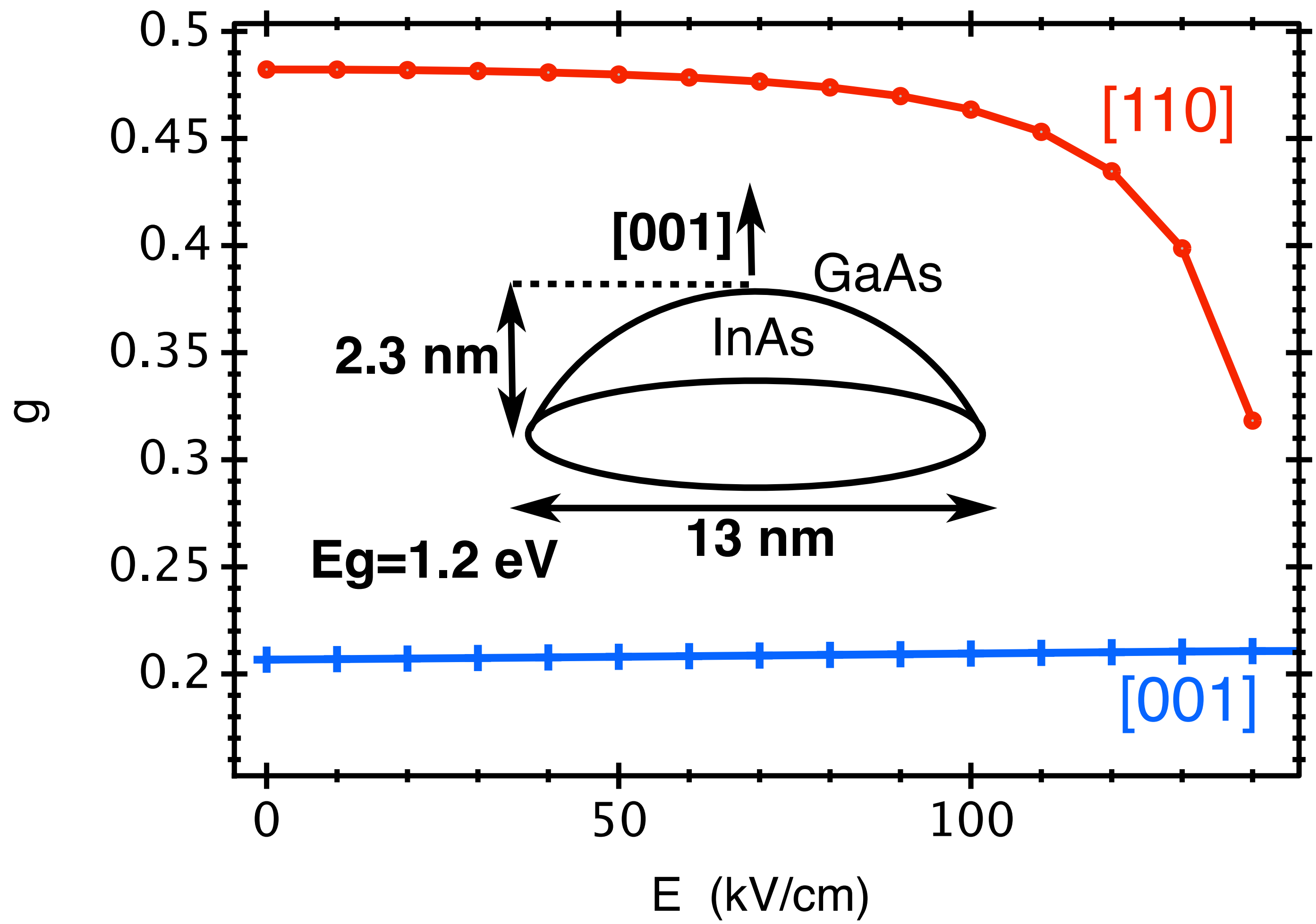

g-TMR

$$H_s = -g\,\frac{\mu_B}{\hbar}\,\vec{B}\cdot\vec{S}$$

$$\rightarrow H_s = -\frac{\mu_B}{\hbar}\,B_\alpha\,g_{\alpha\beta}\,S_\beta$$

$$= \vec{\Omega}\cdot\vec{S}$$

→controllable B_{eff}

g-TMR experiments: quantum wells

Kato et al., *Science* **299**, 1201. (2003)

electric field to modify the electron wavefunction in a parabolic quantum well

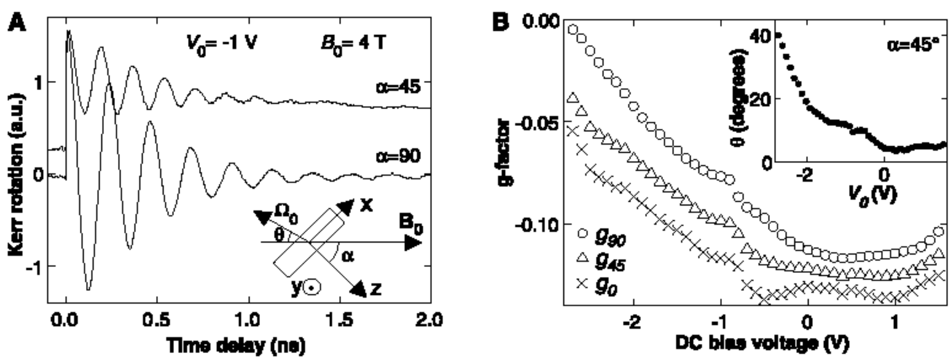

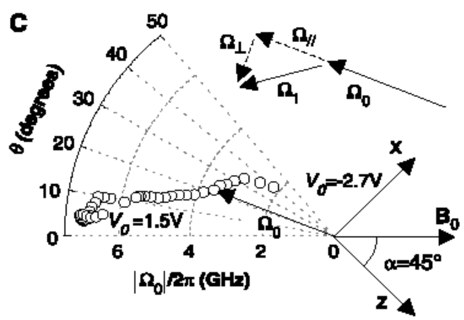

Fig. 2. Measurement of anisotropic g tensor. (A) Representative TRKR scans for $\alpha = 90°$ (Voigt geometry) and $\alpha = 45°$ for $V_0 = -1$ V and $B_0 = 4$ T. Inset shows geometry of experiment. (B) Voltage dependence of g_{90} (open circles) and g_{45} (open triangles) measured at $B_0 = 4$ T along with calculated g_0 (crosses). Inset shows the angle θ between B_0 and Ω_0 as a function of V_0. (C) Voltage-dependent Ω_0 for $B_0 = 4$ T and $\alpha = 45°$. Each Ω_0 is represented by an open circle indicating the endpoint of the precession vector from the origin. Data points are separated by 0.1 V.

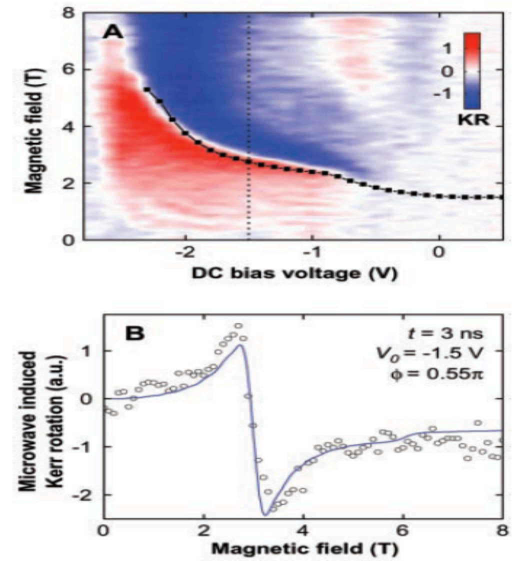

Fig. 3. Demonstration of g-TMR at $\alpha = 45°$. (A) Microwave-induced TRKR as a function of B_0 and V_0 at $t = 3$ ns, $\phi = 0.55\pi$ rad, and $f = 2.660$ GHz. The black squares show the expected positions of resonance, obtained from data similar to that used in Fig. 2B. A device different from that of Fig. 2 was used with qualitatively similar characteristics. In this measurement, the laser wavelength was tuned to 755 nm. The dotted line shows the position where the line cut for Fig. 3B is taken. (B) A line cut along magnetic field axis at $V_0 = -1.5$ V shows a typical g-TMR resonance feature. The blue line represents the results from a numerical simulation of the Bloch equations.

g-TMR in self-assembled InAs/GaAs dots

E: growth direction
B: different directions
different dot heights, elongations

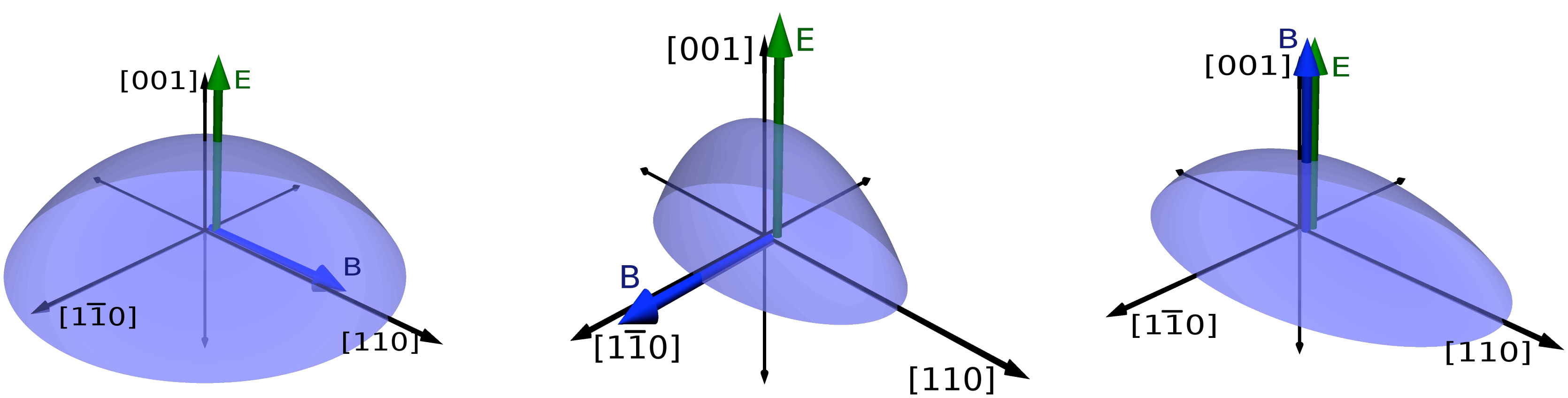

g-TMR in self-assembled InAs/GaAs dots

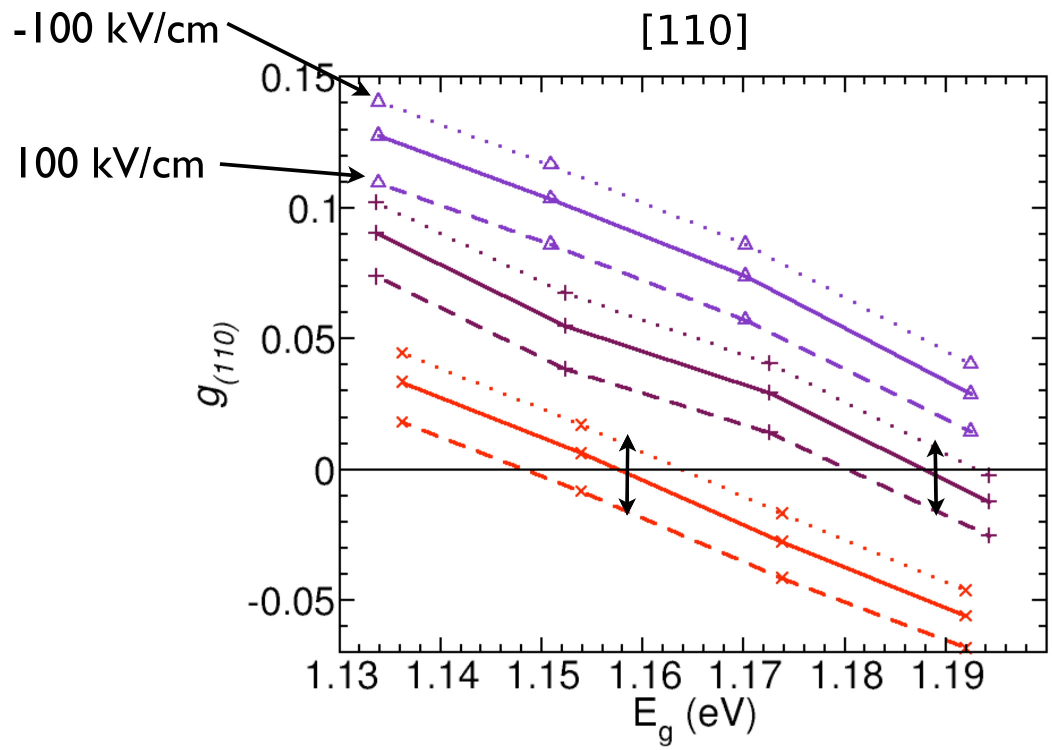

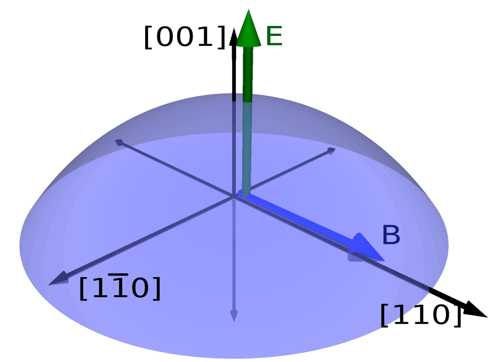

e=1

e=1.25

e=1.67

fixed height,
vary base size

large
dot

small
dot

g-TMR in self-assembled InAs/GaAs dots